Control Engineering Practice 17 (2009) 442–455

Contents lists available at ScienceDirect

Control Engineering Practice

journal homepage: www.elsevier.com/locate/conengprac

Design, tuning, and evaluation of a full-range adaptive cruise control system with collision avoidance

Seungwuk Moon [a], Ilki Moon [b], Kyongsu Yi [c,*]

[a] Program in Automotive Engineering, Seoul National University, 599 Gwanangno, Gwanak-Gu, Seoul 151-742, Korea
[b] Hyundai Motor Company, Jangduk-Dong, Hwaseong, Kyonggi-Do 445-706, Korea
[c] School of Mechanical and Aerospace Engineering, Seoul National University, 599 Gwanangno, Gwanak-Gu, Seoul 151-742, Korea

ARTICLE INFO

Article history:
Received 25 November 2007
Accepted 4 September 2008
Available online 4 November 2008

Keywords:
Adaptive cruise control
Collision avoidance
Warning index
Time-to-collision
Vehicle test

ABSTRACT

This paper describes the design, tuning, and evaluation of a full-range adaptive cruise control (ACC) system with collision avoidance (CA). The control scheme is designed to improve drivers' comfort during normal, safe-driving situations and to completely avoid rear-end collision in vehicle-following situations. Driving situations are divided into safe, warning, and dangerous modes. Three different control strategies have been proposed, depending on the driving situation. The driving situations are determined using a non-dimensional warning index and the time-to-collision (TTC). The control parameters of the proposed ACC/CA system are tuned by a confusion-matrix method using manual-driving data in no-crashing driving situations. The vehicle-following characteristics of the subject vehicle were compared to real-world, manual-driving data. Finally, the ACC/CA system was also implemented in a real vehicle and tested in both safe-traffic and severe-braking situations. It is shown that the proposed control strategy can provide natural following performance that is similar to human manual-driving in both high-speed driving and low-speed stop-and-go situations. Furthermore, it can prevent the vehicle-to-vehicle distance from dropping to an unsafe level in a variety of driving conditions.

1. Introduction

As with adaptive cruise control (ACC), stop-and-go (SG), lane-keeping support, collision warning and collision avoidance (CW/CA), assisted lane change, and automated parking assistance, advanced driver assistance systems (ADAS) have been extensively researched; further, several developments have transpired since the 1990s (Börner & Isermann, 2006; Fancher, Bareket, & Ervin, 2000 ; Fancher, Bareket, Ervin, & Peng, 2004; Iljima et al., 2000; Shladover, 1991; Wang & Rajamani, 2004). ADAS are believed to reduce the risk of accidents, improve safety, and enhance comfort and performance for drivers. One of the developments in cruise control technology in present-day cars is ACC systems, which can detect the preceding vehicle and automatically accelerate and decelerate the vehicle to maintain a specified space between the two vehicles. While several automakers have already introduced features such as ACC in their top-of-the-line cars, many others are pursuing research to introduce ACC and other advanced features, such as collision warning and avoidance systems, into their products.

Since ACC and CW/CA systems always work with a co-existing human driver, they can be useful to the driver and their control logic and operational characteristics need to be similar to the decision-making and driving characteristics of the human driver. Recently, several researchers have focused their research on manual-driving behavior and its application to the human-centered design of ACC and/or CW/CA systems (Fancher et al., 2000; Goodrich & Boer, 2003; Peng, 2002; Vahidi & Eskandarian, 2003). Human-driver driving behavior has been analyzed in various scenarios. Based on the analysis, a control system that is capable of accurately modeling this behavior has been constructed to provide natural vehicle behavior during low-speed driving (Venhovens et al., 2000). Time gap and the time-to-collision (TTC) have been used in the analysis of driving behavior of a driver who is following a preceding vehicle (Fancher et al., 2000). Driver behavior in adjusting the clearance during vehicle-following has been analyzed by focusing on the target clearance deviation for application to an ACC design. A longitudinal driver model that was developed based on measured driving data and the evaluation of the impact of ACC vehicles on traffic flow was presented by Peng (2002). Drivers' crash-avoidance behavior and the effect of ABS on drivers' ability to avoid a collision in a crash-imminent situation were reported by Larson and Fowler (2005). Although many research results on ACC and CW/CA systems have

* Corresponding author. Tel.: +82 2 880 1941; fax: +82 2 880 0561.
E-mail address: kyi@snu.ac.kr (K. Yi).

0967-0661/$ - see front matter © 2008 Elsevier Ltd. All rights reserved.
doi:10.1016/j.conengprac.2008.09.006

been published, little has been published on the integrated design of a full-range ACC system with a CA system. In addition, different cruise control strategies have been proposed to address the problem of passenger safety and comfort (Vahidi & Eskandarian, 2003). However, some work still needs to be done about the possibility of making vehicles capable of autonomous reactions to normal and emergency driving situations.

To integrate ACC and CA systems, this paper proposes a longitudinal controller that consists of index-based control modes and scheduling of acceleration with respect to control modes. The proposed control strategy enables a subject vehicle to operate in three control modes: 'ACC', 'ACC+CA', and 'CA'. The developed control modes are determined by two indexes. One has been developed in our previous research and the other is well-known in collision warning/avoidance systems. In addition, this paper proposes a tuning method of using manual-driving data in no-crash driving situations, including comfort-driving and severe-braking situations. Since it is important to select the parameters that are related to the transitions between the three control modes, parameters of the proposed controller are tuned using a confusion matrix and manual-driving data under no-crashing. Finally, the performance of the proposed control algorithm is verified through computer simulation and vehicle tests in high-mu (high tire–road friction) road conditions. Although the proposed control strategy for full-range ACC with CA has been evaluated for high-mu road conditions, it has been designed to incorporate the effect of even low tire–road friction.

2. Design of a full-range adaptive cruise control system with collision avoidance

Fig. 1 shows the scheme of the proposed ACC/CA system. As shown in Fig. 1, the ACC/CA system consists of upper-level and lower-level controllers. The upper-level controller uses the longitudinal velocity, relative distance, and relative velocity. These measurements are used to calculate indexes and the desired acceleration. Based on the calculated indexes, the upper-level controller determines driving situations that are classified as: 'safe', 'warning', and 'dangerous'. In line with the driving situation, it determines the control input, which is the desired acceleration. The lower-level controller manipulates a throttle or brake actuator so that the acceleration of the vehicle tracks a desired acceleration. It uses the longitudinal acceleration, wheel speeds, engine RPM, turbine speed, and gear status. The engine RPM, turbine speed, and gear status are used to calculate the desired engine torque. The longitudinal acceleration is used to track the desired acceleration through feedback control. In short, the control principles of the throttle or brake are based on reverse dynamics, and a feed-forward/proportional-integral-derivative (PID) control principle is also used. A throttle angle is computed from the desired engine torque using an engine map and a torque-converter map. In addition, the brake pressure is obtained from the total brake torque which is computed from the motion of the vehicle. Throttle-brake switching is determined by using a switching line that is obtained from data on zero-throttle acceleration of the vehicle. When the desired acceleration for a given vehicle velocity is greater than the switching line, the throttle-control principle is applied. On the other hand, when the desired acceleration is smaller than the switching line, the brake-control principle is applied. Details of the lower-level controller are described by Han and Yi (2006).

2.1. Indexes for driving conditions

In this study, a non-dimensional warning index and an inverse TTC are used to determine driving situations. Most of the existing CA/CW systems use a similar algorithm based on the braking-critical distance and the warning-critical distance (Seiler, Song, & Hedrick, 1998). The non-dimensional warning index developed in our previous research (Yi, Woo, Kim, & Lee 1999) represents the danger of physical collision in the current driving situation and is defined as follows:

$$x = \frac{c - d_{br}}{d_w - d_{br}} \tag{1}$$

In (1), c is the actual vehicle spacing, and d_{br} and d_w are the braking-critical and warning-critical distances, respectively. If c exceeds d_{br} and d_w, then the warning index is a positive value that is greater than unity and indicates that the current driving

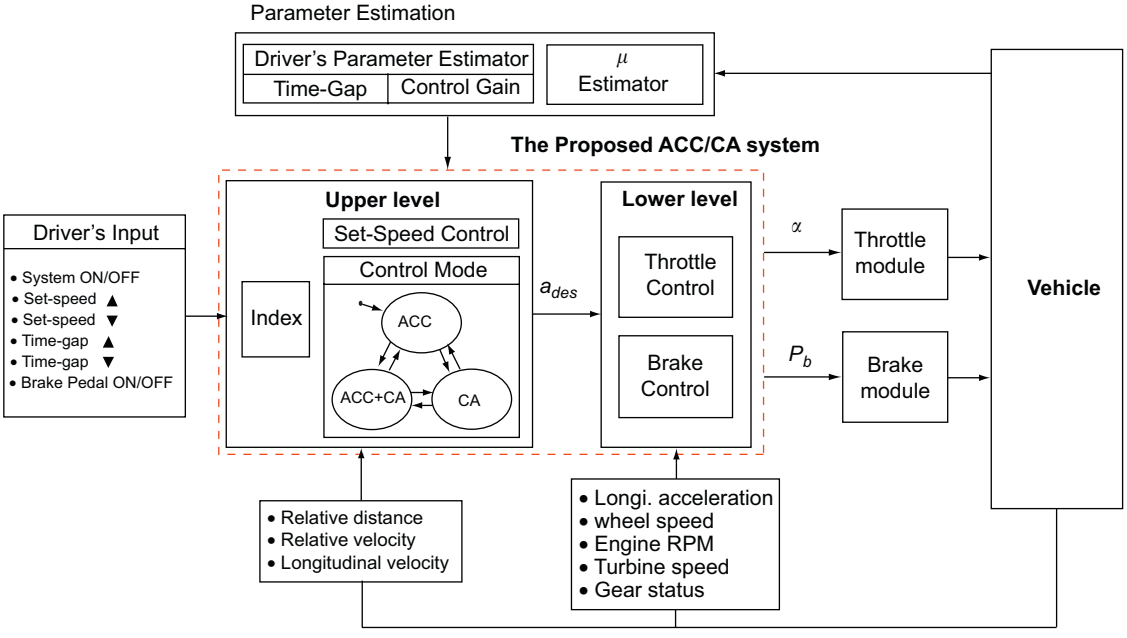

Fig. 1. Scheme of a full-range ACC system with a CA system.

situation is in a safe region. If c is below d_{br}, then the warning index is a negative value and indicates that the current driving situation can be dangerous. The warning-critical and braking-critical distances are defined as follows:

$$d_{br} = v_{rel}T_{s,delay} + f(\mu)\left(\frac{v_s^2 - (v_s - v_{rel})^2}{2a_{max}}\right)$$
$$d_w = v_{rel}T_{s,delay} + f(\mu)\left(\frac{v_s^2 - (v_s - v_{rel})^2}{2a_{max}}\right) + v_s T_{h,delay} \quad (2)$$

In (2), $v_{rel}(=v_s - v_p)$ is the relative velocity between the subject vehicle and the preceding vehicle, $T_{s,delay}$ is the system delay, which is given by the brake-system hardware, a_{max} is the maximum deceleration of the vehicle under normal road conditions, v_s is the velocity of the subject vehicle, $T_{h,delay}$ is the delay in human response between recognition and manipulation, $f(\cdot)$ is the friction scaling function, and μ is the estimated value of the tire–road friction coefficient. These terms can be derived from the kinematics of the two vehicles that brake to a full stop. If the vehicles start at this distance and brake with their maximum decelerations, they will come to a stop with their bumpers touching each other. To make the critical distance more conservative, two delay terms are added; these account for system and driver delays. From Eqs. (1) and (2), it is shown that the warning index can be influenced by the friction scaling function; further, the tire–road friction coefficient will be used to scale the critical distances. A piece-wise linear function of the following form is used for the friction scaling function, $f(\cdot)$ (Yi et al., 1999):

$$f(\mu) = \begin{cases} f(\mu_{min}) & \text{if} \quad \mu \leqslant \mu_{min} \\ f(\mu_{min}) + \dfrac{f(\mu_{norm}) - f(\mu_{min})}{\mu_{norm} - \mu_{min}}(\mu - \mu_{min}) & \text{if} \quad \mu_{min} < \mu < \mu_{norm} \\ f(\mu_{norm}) & \text{if} \quad \mu_{norm} \leqslant \mu \end{cases} \quad (3)$$

In (3), μ_{norm} is the normal friction coefficient and μ_{min} is the smallest friction coefficient to be considered. $f(\mu_{norm})$ is set to unity and $f(\mu_{min})$ is set to 'μ_{norm}/μ_{min}' because there should be no distance scaling when the friction coefficient is equal to its normal value. In this study, the parameters for the warning index and friction scaling are: $\mu_{norm} = 0.9$, $\mu_{min} = 0.2$, and $a_{max} = 8\,\text{m/s}^2$. Eq. (2) confirms that when the tire–road friction coefficient decreases, the braking-critical and the warning-critical distances increase. Since the tire–road friction coefficient is needed to calculate the warning index, it is assumed that information on the tire–road friction coefficient can be obtained by various methods or the real-time estimation of the tire–road friction.

The steady-following is defined as a following situation at a small relative velocity. The inverse of the time-to-collision (TTC^{-1}) is used to define the driver's steady-following situation in this study. The TTC, which is a well-known parameter in CW/CA systems, is defined as

$$\text{TTC} = \frac{c}{v_s - v_p} \quad (4)$$

In (4), as before, v_p is the preceding vehicle's velocity and v_s is the subject vehicle's velocity. In the case where the preceding vehicle's velocity is constant, the subject vehicle's speed converges to the preceding vehicle's speed and the subject vehicle follows the preceding vehicle at a nearly constant distance. Therefore, the steady-following of a human driver can be defined as a situation with a small value of the inverse of the TTC. If the inverse TTC is positive, it indicates that the subject vehicle is moving too close to the preceding vehicle. The inverse TTC is related to the visual cues that might guide driver headway

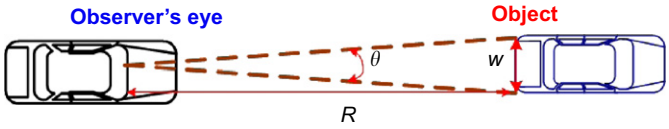

Fig. 2. The looming effect.

maintenance. The concept of looming, as described in human-factor studies, is employed in the analysis of human perception and longitudinal control behavior in driving situations. The looming effect was first investigated by Hoffmann and Mortimer (1996) and was a key factor in the human-centered design of an ACC-with-braking and forward-crash-warning system undertaken by Fancher et al. (2000). As illustrated in Fig. 2, the size of the image that is projected onto the eye of the following driver depends on the range of the observed object, i.e., the preceding vehicle. If there is relative motion between the vehicles, the range, R, and the angle, θ, will change.

The width of the preceding vehicle, w, is constant and can be represented as

$$w = R\theta \quad (5)$$

The rate of change of the range is related to the rate of change of the angle, θ, which is occluded by the image as projected onto the observer's eye, i.e., the driver's eye, as follows:

$$\frac{dw}{dt} = 0 = \dot{R}\theta + R\dot{\theta} \quad (6)$$

The looming effect is represented by the ratio of the occluded angle to the rate of change of that angle, i.e. $\theta/\dot{\theta}$. Therefore, the looming effect can be represented as

$$\frac{\theta}{\dot{\theta}} = \frac{R}{-\dot{R}} = \frac{c + l}{v_{rel}} \approx \text{TTC} \quad (7)$$

In Eq. (7), c is the clearance between the vehicles, v_{rel} is the relative velocity between the subject and preceding vehicles, and l is the distance between the front bumper and the driver's eye. As shown in Eq. (7), the driver's sensation of looming is related to the inverse TTC, which is computed using the range and the rate of change of the range.

Generally speaking, a driver executes three behaviors while driving a vehicle: perception, decision, and manipulation. In this study, the driver's perception of the preceding vehicle's motion, in relation to the subject vehicle, is represented as two indexes, the warning index and the inverse TTC. The result of decision and manipulation of the driver for the given driving situation is considered to be the resultant acceleration of the subject vehicle. In this context, relationships between the warning index and the deceleration of the subject vehicle have been investigated using manual-driving data. Further, relationships between the inverse TTC and the deceleration of the subject vehicle have been investigated. To investigate the relationships between each index and the deceleration of the subject vehicle, severe-braking test data were collected under high-mu road conditions and analyzed together with normal-driving data. Fig. 3 shows the test vehicle used in this study. Manual-driving data were collected in a highway, a perimeter road, and urban area. The duration of each test datum varies between 40 and 1800 s, and the velocity varies between 0 and 120 km/h. The number of measured data in normal-driving situations is 1809 over 125 drivers, and the number of measured data in severe-braking situations is 62 for experienced drivers.

The mean and percentile values of the warning index and the inverse TTC are computed for ranges of deceleration. Comparisons of the warning index and the inverse TTC for four ranges of deceleration are given in Tables 1 and 2, respectively. As

illustrated in these two tables, the magnitude of the warning index significantly decreases and the inverse TTC increases as the vehicle's deceleration increases. This implies that the driver's perception, decision, and manipulation cause large deceleration as the warning index decreases and/or the inverse TTC increases. The mean, the 5th percentile, and the 95th percentile values of the warning index and the inverse TTC for alternative ranges of deceleration are compared in Fig. 4. Therefore, the warning index and the inverse TTC can be used to determine a driving situation.

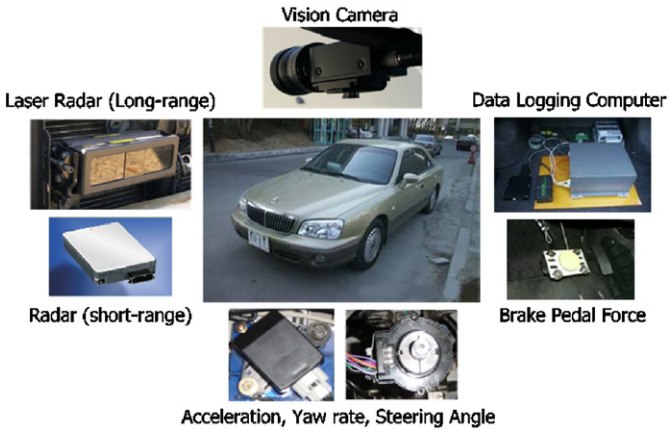

Fig. 3. Test vehicle for logging driving data.

Table 1
Warning indexes (x) for various ranges of deceleration

Acceleration/ percentile (m/s^2)	5%	25%	Mean	75%	95%
$-2<a<-0.5$	0.52	0.93	1.41	1.57	1.86
$-4<a<-2$	0.41	0.63	0.98	1.34	1.60
$-6<a<-4$	0.23	0.28	0.82	0.98	1.50
$a<-6$	−0.56	0.02	0.13	0.31	0.45

Table 2
Inverse TTC (s^{-1}) values for various ranges of deceleration

Acceleration/ percentile (m/s^2)	5%	25%	Mean	75%	95%
$-2<a<-0.5$	−0.02	0.03	0.11	0.17	0.36
$-4<a<-2$	−0.01	0.13	0.25	0.34	0.60
$-6<a<-4$	0.23	0.28	0.70	0.98	1.50
$a<-6$	0.56	0.85	1.13	1.35	1.72

2.2. Driving situations and control modes

In manual driving for 125 people, 98% of the accelerations were between −2.17 and 1.77 m/s^2 (Moon & Yi, 2008). Most drivers and passengers feel significantly uncomfortable when the vehicle deceleration is greater than 3–4 m/s^2 (in absolute value). Drivers use large deceleration (greater than 4 m/s^2 in absolute value) only when they really need to apply severe braking to prevent the vehicle-to-vehicle distance from dropping to an unsafe level. In this context, driving situations can be evaluated using the vehicle acceleration. In this study, when the vehicle deceleration is smaller than 2 m/s^2 (in absolute value), the driving situation is considered to be a 'safe situation'. When the absolute magnitude of the vehicle deceleration is greater than 4 m/s^2, the driving situation is considered to be a 'severe braking or dangerous situation'. The driving situations are divided into: comfort-mode (Mode-1), large-deceleration mode (Mode-2), and severe-braking situation (Mode-3), as follows:

$$\begin{aligned}&\text{Mode-1 (comfort mode)}: \quad a > -2\ m/s^2\\ &\text{Mode-2 (large deceleration mode)}: \quad -2\ m/s^2) \geqslant a > -4\ m/s^2\\ &\text{Mode-3 (severe braking mode)}: \quad -4\ m/s^2 \geqslant a\end{aligned} \tag{8}$$

As shown in Fig. 5, the driving situations can be analyzed in a two-dimensional graph of the warning index vs. the inverse TTC. When the warning index is high and the inverse TTC is low, the driving situation is in a safe region. However, if the warning index decreases or the inverse TTC gradually increases, the danger of a rear-end collision increases and the vehicle needs to quickly decelerate to avoid the warning region. When the warning index is low and the inverse TTC is high, the driving situation is critical and therefore, the emergency brake should be applied.

The relationship between indexes and control modes are defined as follows:

$$\begin{aligned}&(x \geqslant \alpha_1 \text{ and } \mathrm{TTC}^{-1} \leqslant iT_1) \Rightarrow \text{Control Mode-1, ACC}\\ &(x < \alpha_1 \text{ or } iT_1 < \mathrm{TTC}^{-1}) \Rightarrow \text{Control Mode-2, ACC} + \text{CA}\\ &(x \leqslant \alpha_2 \text{ and } iT_2 < \mathrm{TTC}^{-1}) \Rightarrow \text{Control Mode-3, CA}\end{aligned} \tag{9}$$

In (9), α_1 and α_2 are the warning-index thresholds and iT_1 and iT_2 are the inverse TTC thresholds. It is important to select

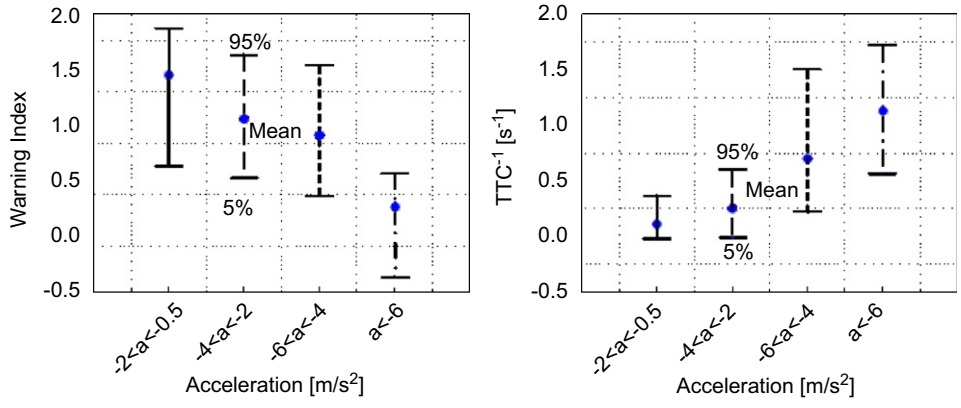

Fig. 4. Analysis of the warning index and inverse TTC for various rates of deceleration.

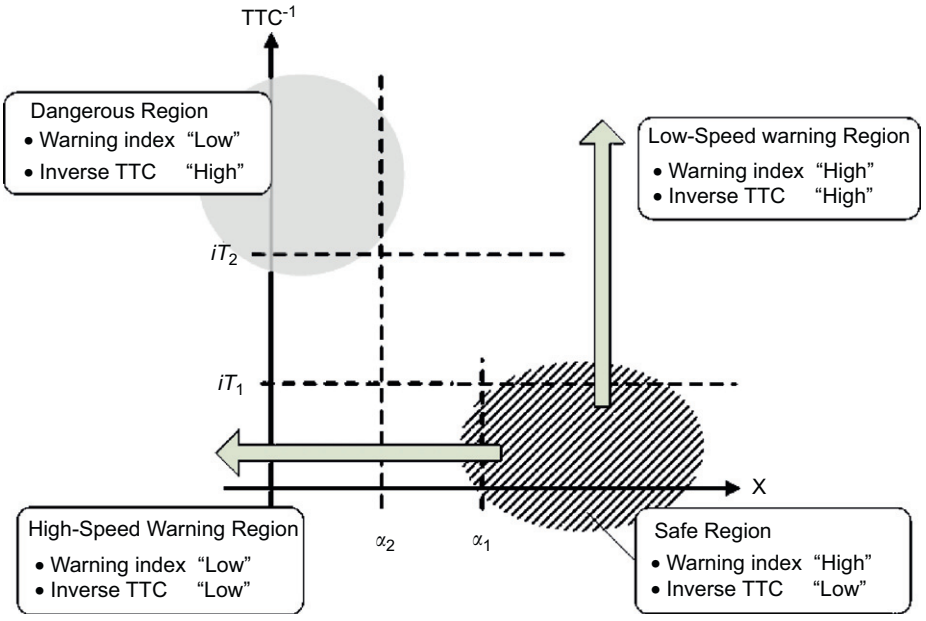

Fig. 5. The warning index and the inverse TTC for various driving situations.

appropriate threshold values for the warning index and the inverse TTC that are acceptable to drivers and that improve safety. For example, frequent warning and braking are likely to annoy the driver and are therefore, unnecessary. On the other hand, less-sensitive warning and braking may cause the driver to feel unsafe. Therefore, the parameters in expression (9) for transition of the control mode should be based on manual-driving data in no-crash driving situations. Firstly, the desired acceleration of the subject vehicle has been designed according to a control mode. Secondly, threshold values for the control modes are tuned using manual-driving data in no-crashing driving situations.

2.3. Design of the desired acceleration for control modes

Basically, linear optimal control theory has been used to design the desired acceleration in normal vehicle-following situations. Using integrators to model the vehicles, a state-space model for the controlled and preceding vehicles can be written as follows:

$$\dot{x} = Ax + Bu + \Gamma w = \begin{bmatrix} 0 & -1 \\ 0 & 0 \end{bmatrix} x + \begin{bmatrix} 0 \\ -1 \end{bmatrix} u + \begin{bmatrix} \tau \\ 1 \end{bmatrix} w \tag{10}$$

In Eq. (10), τ is the linear coefficient, i.e., the time gap. The states are $x^{\mathrm{T}} = [x_1 x_2] = [c_d - c v_p - v_s]$, the input, u, is the subject vehicle's acceleration, and the disturbance, w, is the preceding vehicle's acceleration. c_d and c are the desired clearance and actual clearance between the preceding and subject vehicles, and v indicates velocity. Subscripts, p and s, indicate the preceding and the subject vehicles, respectively. The control of the ACC/CA vehicle can be seen as a linear-quadratic optimization problem, namely, the design of the state-feedback control principle for minimizing the following-distance error and the speed error, and the control input:

$$J = \int_0^\infty (x^{\mathrm{T}} Q x + u^{\mathrm{T}} R u)\, \mathrm{d}t \tag{11}$$

The weighting matrices, Q and R, are defined as follows:

$$Q = \begin{bmatrix} \rho_1 & 0 \\ 0 & \rho_2 \end{bmatrix}, R = [r]. \tag{12}$$

The gains for the state-feedback principle, $u = -Kx$, are chosen to minimize the cost function. The desired acceleration of the subject vehicle can be determined by solving Eq. (11). According to Lyapunov's second method and Riccati equation:

$$A^{\mathrm{T}} P + PA - PBR^{-1} B^{\mathrm{T}} P + Q = 0 \tag{13}$$

The coefficient matrix K can be obtained by

$$K = R^{-1} B^{\mathrm{T}} P \tag{14}$$

In Eq. (14), P is the positive-definite steady-state solution of the Riccati equation. Therefore, the desired acceleration is represented by

$$a(t) = u(t) = -Kx = -k_1(v_s(t))(c_d(t) - c(t)) - k_2(v_s(t))(v_p(t) - v_s(t)) \tag{15}$$

In Eq. (15), $k_1(\cdot)$ and $k_2(\cdot)$ are the control gains as a function of the subject vehicle's speed, $v_s(t)$, and have been obtained by tuning the weighting matrices, Q and R. Since the weighting matrices, Q and R, impact on the performance of this following-system, the weighting factors, ρ_1, ρ_2, and r, have been chosen to achieve naturalistic behavior of the subject vehicle that would seem natural to a human driver in normal-driving situations. In this study, alternative weighting factors have been used for low-, medium-, and high-speed ranges. For 'Control Mode-1,' the desired acceleration is represented by

$$a_{des}(t) = \begin{cases} a_{max}(v_s(t)) & \text{if} \quad a(t) > a_{max}(v_s(t)) \\ a(t) & \text{if} \quad a_{min}(v_s(t)) \leqslant a(t) \leqslant a_{max}(v_s(t)) \\ a_{min}(v_s(t)) & \text{if} \quad a(t) < a_{min}(v_s(t)) \end{cases} \tag{16}$$

As shown in Eq. (16), the desired acceleration is restricted by the maximum and minimum acceleration, $a_{max}(\cdot)$ and $a_{min}(\cdot)$ to improve ride comfort. $a_{max}(\cdot)$ and $a_{min}(\cdot)$ are based on the statistical analysis of the manual-driving data of 125 drivers. Fig. 6 shows the 5th and 95th percentile values of the driver's acceleration for every increment of 10 km/h in the speed. As illustrated in Fig. 6, manual-driving data for normal vehicle-following situations show that drivers use relatively large acceleration in low-speed, vehicle-following situations.

Based on the statistical analysis shown in Fig. 6, the velocity-dependent acceleration limitations, $a_{max}(\cdot)$ and $a_{min}(\cdot)$, are determined as shown in Fig. 7(a). The desired acceleration is computed using the velocity-dependent optimal gain and restricted by the acceleration limit, as shown in Fig. 7(a). The control gains for low-speed driving situations are determined by Eq. (14) to obtain good vehicle-following performance with these weighting factors: $\rho_1 = 1$, $\rho_2 = 6$, and $r = 8$. Since in the case of high-speed driving situations ride comfort is a more important factor in preceding vehicle following, the control gains are designed to obtain smooth vehicle behavior with following weighting factors: $\rho_1 = 1$, $\rho_2 = 6$, and $r = 18$. The control gains, $k_1(\cdot)$ and $k_2(\cdot)$, for the medium range of speed, are determined to obtain smooth transitions between low- and high-speed driving conditions. The velocity-dependent control gains, $k_1(\cdot)$ and $k_2(\cdot)$, are shown in Fig. 7(b). All the control gains used in this study are designed towards naturalistic behavior of the subject vehicle similar to the behavior of manually driven vehicles in normal-driving situations.

As shown in Eq. (15), the desired clearance, c_d, is needed to compute the desired acceleration. In this study, the desired clearance defined by Eq. (17) has been used:

$$c_d = c_0 + \tau v_p \tag{17}$$

In Eq. (17), c_0 is the zero-speed clearance and τ is the linear coefficient. The zero-speed clearance and the linear coefficient can be adapted to make the steady-state following characteristics of an ACC/CA vehicle similar to that of a manually driven vehicle. A recursive, least-squares method for adapting the zero-speed clearance and the linear coefficient of human drivers during manual driving (i.e., with the ACC is turned off) has been proposed by Yi and Moon (2004). The design parameters of the cruise control principle, c_0 and τ, can be tuned to suit the driver.

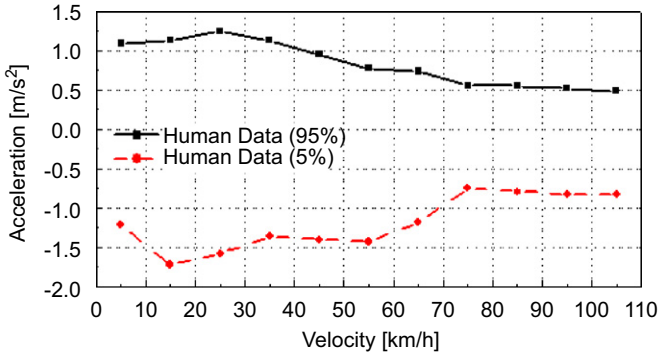

Fig. 6. Acceleration analysis of manual-driving data over 125 drivers in following vehicles.

In the case of 'Control Mode-2,' the desired acceleration is computed in the same manner as for 'Control Mode-1' and the deceleration limit is extended to $-4\,\mathrm{m/s^2}$; refer Eq. (18). This implies that the desired acceleration of this mode can be larger than that of 'Control Mode-1' for improving safety:

$$a_*(t) = -k_1(v_s(t))(c_d(t) - c(t)) - k_2(v_s(t))(v_p(t) - v_s(t))$$
$$a_{des}(t) = \begin{cases} a_*(t) & \text{if } a_*(t) > -4\,\mathrm{m/s^2} \\ -4\,\mathrm{m/s^2} & \text{else} \end{cases} \tag{18}$$

As with 'Control Mode-1,' the desired clearance, c_d, is defined by Eq. (17).

In the case of 'Control Mode-3', the desired acceleration, a_{des}, is computed by using non-linear functions that map the indexes to the desired accelerations. The functions, $f_1(\cdot)$ and $f_2(\cdot)$, are obtained by using the confusion-matrix method on manual-driving data in no-crash driving situations, including comfort-driving and severe-braking situations. As shown in Fig. 8, the function, $f_1(\cdot)$, is a table that represents the relationship between the warning index and the deceleration of the vehicle while $f_2(\cdot)$ is a table that represents the relationship between the inverse TTC and the deceleration of the vehicle. These tables will be explained in the following section. From the investigation of manual-driving data, it is found that the warning index is closely related to the driver's decisions and to the vehicle-acceleration behavior in medium- and high-speed driving situations and to the inverse TTC in low-speed driving situations. These facts have been incorporated into the design of the desired vehicle acceleration, a_{des}, in severe-braking situations. The desired acceleration is computed as

$$a_{**}(t) = W_1(v_s(t))f_1(x) + W_2(v_s(t))f_2(\mathrm{TTC}^{-1})$$
$$a_{des}(t) = \begin{cases} a_{**}(t) & \text{if } a_{**}(t) > -8\,\mathrm{m/s^2} \\ -8\,\mathrm{m/s^2} & \text{else} \end{cases} \tag{19}$$

In Eq. (19), W_i is the weighting factor, which is defined as a function of the vehicle speed. The computation of the desired acceleration in severe-braking situations is illustrated in Fig. 8.

As shown in Fig. 8, the weight function is used to develop a non-linear function for the warning index and the inverse TTC. In general, the steady-following is defined as a following situation that maintains a specified distance at a small relative velocity ($v_{rel} \approx 0$). In the case of steady-following, the warning index in high-speed driving is smaller than that in low-speed driving. Since the warning and braking distances tend to increase as the subject vehicle's velocity increases, Eqs. (1) and (2) imply that the denominator of the warning index, $c - d_{br}$, increases while the numerator, $d_w - d_{br}$, decreases. This implies that the warning index can be sensitive in high-speed driving. In the case of steady-following, the inverse TTC becomes very small. However, if there is relative motion between the vehicles, the inverse TTC will

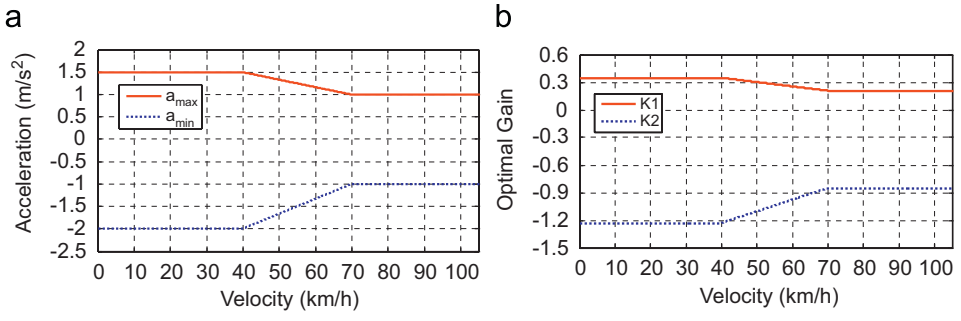

Fig. 7. Velocity-dependent control gain and range of acceleration. Legend: upper boundary = a_{max}; lower boundary = a_{min}.

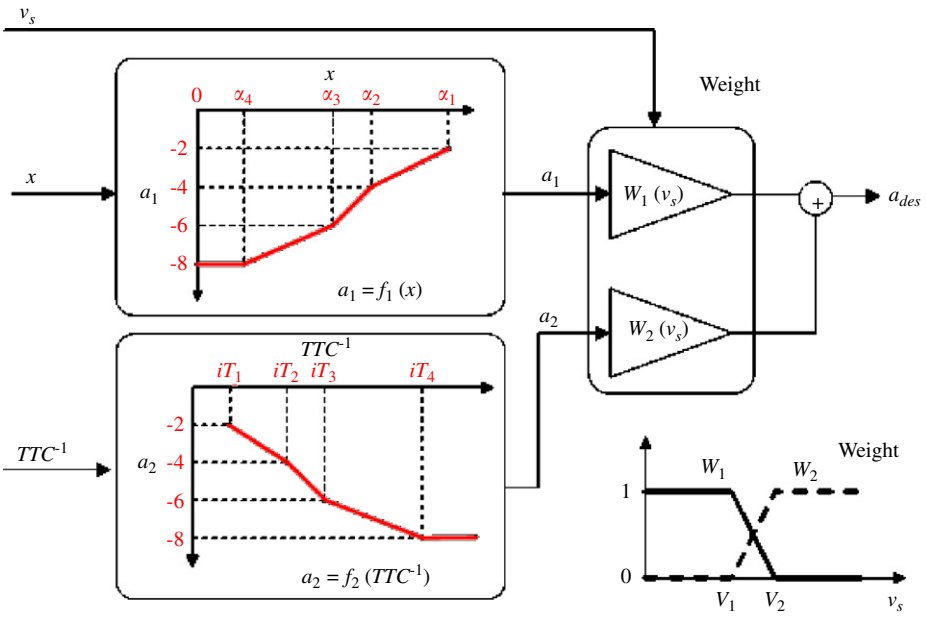

Fig. 8. Design of the desired acceleration in severe-braking situations.

change. As shown in Eq. (2), if the relative velocity is identical, the clearance, c, will influence the inverse TTC. As a human driver tends to maintain a large clearance in high-speed driving, the inverse TTC in high-speed driving can be smaller than that in low-speed driving. Therefore, the inverse TTC can be sensitive in low-speed driving. In this context, the weight function is established as shown in Fig. 8.

In the case of 'Control Mode-2,' the desired acceleration is computed as for 'Control Mode-1' and the acceleration limit is extended to $-4\,m/s^2$. As the warning index decreases and the inverse TTC increases, the desired acceleration in 'Control Mode-2' is smaller. Since those indexes are defined as functions of the vehicle-to-vehicle clearance and the relative velocity, the desired acceleration is smaller depending on the driving situation. However, since the minimum desired acceleration in 'Control Mode-2' is $-4\,m/s^2$, the control mode must be changed for applying a larger deceleration to the subject vehicle. When the warning index and the inverse TTC exceed the threshold values of the indexes, α_2 and iT_2, the control mode switches to 'Control Mode-3' and the desired acceleration of 'Control Mode-3' is applied. In the case of 'Control Mode-3', since the warning index is smaller than α_2 and the inverse TTC is bigger than iT_2, the maximum value of the desired deceleration, $W_1f_1(\alpha_2)+W_2f_2(iT_2)$, is $-4\,m/s^2$. Depending on the change of indexes, either the control mode is switched or a larger deceleration, which is greater than $4\,m/s^2$ in absolute value, is computed using non-linear functions. In short, since the threshold values (α_2 and iT_2) and the non-linear function-map of 'Control Mode-3' are based on an identical relationship between indexes and deceleration, a smooth transition is expected during a change in the control mode. In addition, since the desired acceleration is computed using the warning index and the inverse TTC and those indexes are defined as functions of the vehicle-to-vehicle clearance and the relative velocity, the desired acceleration is, in turn, represented by a non-linear function of the clearance and the relative velocity. The selection of the thresholds for the control modes and the design of the non-linear functions $f_1(\cdot)$ and $f_2(\cdot)$, are described in more detail in Section 2.4. The bandwidths of the inner acceleration-loop vary between 0.2 and 0.5 Hz, depending on the control modes. The bandwidths of the outer controller-loop for the clearance and velocity control vary between 0.06 and 0.18 Hz, depending on the control modes. In this study, the sampling intervals for the upper- and lower-level controllers are 50 and 10 ms, respectively.

2.4. Manual-driving data-based tuning of control mode thresholds

Generally, human factors are crucial for vehicles with ACC systems and are of primary importance in the development of CW/CA systems. In this context, it is important to tune the parameters in integrated ACC/CA systems. To be acceptable by a human driver, the parameters for transition of the control mode (namely, the threshold values) should be determined based on manual-driving data in no-crash driving situations, including comfort-driving and severe-braking situations. The driving situation that is recognized by the human driver is related to the vehicle deceleration that is used by the driver. In the case of ACC/CA controllers, the driving situation is determined through two indexes, the warning index and the inverse TTC. Therefore, it is necessary to investigate a relationship between these two indexes and the deceleration level to find the threshold values for the three control modes. In other words, for a given level of deceleration, we have to find the best-fitting warning index and inverse TTC among possible values. As stated above, the driving situations are divided based on the level of vehicle deceleration into three categories: comfort-mode ($a>-2$), large-deceleration mode ($a>-4$), and severe-braking situation ($a<-4$). Therefore, α_1 and iT_1 are the best-fitting warning index and inverse TTC values for $-2\,m/s^2$. Also, α_2 and iT_2 are the best-fitting values for $-4\,m/s^2$. In this context, a confusion matrix (Lee & Peng, 2004) is used to determine the threshold values for the warning index and the inverse TTC in Eq. (9), besides α_1, α_2, iT_1, and iT_2. The confusion matrix contains information about actual and predicted classifications. In the case of the actual classification, the "More Safe" and "More Threatening" datasets are defined based on the level of deceleration that is employed by the human driver. For example, if the level of deceleration of the subject vehicle is smaller than

$-2\,m/s^2$, the corresponding data that are sampled are classified as "More Threatening." In the case of the predicted classification, the "More Safe" and "More Threatening" datasets are defined based on the warning index and the inverse TTC. If the warning index is smaller than the threshold value, the corresponding data that are sampled are classified as "More Threatening;" the inverse TTC works in the opposite manner. As shown in Fig. 9, *A*, *B*, *C*, and *D* are the number of sampled data in the corresponding regions among the total dataset. '*A*' is the number of correct predictions that an instance is "More Safe" among all the instances in the complete manual-driving dataset. '*B*' is the number of incorrect predictions that an instance is "More Safe." '*C*' is the number of incorrect predictions that an instance is "More Threatening". '*D*' is the number of correct predictions that an instance is "More Threatening".

A performance index is needed to find the most appropriate threshold value for each reference deceleration. The performance index is used as a cost function, namely, the geometrical mean of the true positive (TP) and the precision (P). The geometric mean of *TP* and *P* is defined as Eq. (20) and tends to balance the two objectives of detecting threatening situations and avoiding false alarms:

$$g\_mean_1 = \sqrt{TP\,P}\ (\%)$$
$$TP = \left(\frac{D}{C+D}\right), \quad P = \left(\frac{D}{B+D}\right) \tag{20}$$

For a given reference acceleration, a, the warning-index threshold values, $x_{th}(a)$, and the inverse TTC threshold values, $iT_{th}(a)$, are computed as follows:

$$x_{th}(a) = arg\max_{x}\{\sqrt{TP\,P}\}$$
$$iT_{th}(a) = arg\max_{iT}\{\sqrt{TP\,P}\} \tag{21}$$

In other words, $x_{th}(a)$ and $iT_{th}(a)$ are the warning index and the inverse TTC that maximize the performance index among the possible warning indexes and inverse TTCs, respectively. The g_mean_1 that is computed for reference acceleration values, i.e., -2, -4, and $-6\,m/s^2$, with the warning index and the inverse TTC as the prediction variables are shown in Figs. 10 and 11, respectively. The threshold values obtained from the confusion-matrix method are summarized in Table 3. The driving situation is considered to be a severe-braking situation when either the warning threshold, x_{th}, is smaller than 0.81 or the inverse TTC threshold, iT_{th}, is greater than 0.49. A driving situation is considered to be a normal following situation when neither the warning threshold, x_{th}, is smaller than 1.19 nor the inverse TTC

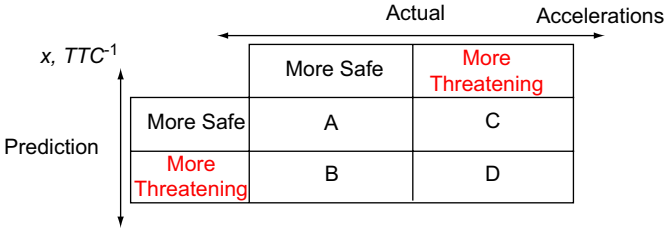

Fig. 9. Confusion-matrix threshold of the warning index and the inverse TTC.

Table 3
Threshold values for the warning index and the inverse TTC

Acceleration (m/s^2)	Warning index	Inverse TTC
−2	1.19	0.21
−4	0.81	0.49
−6	0.65	0.68

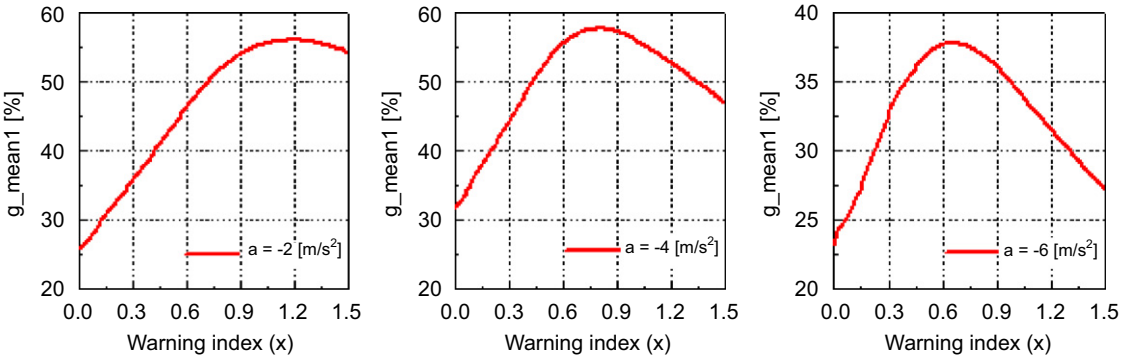

Fig. 10. g_mean_1 computed for three acceleration values (-2, -4, and $-6\,m/s^2$) with the warning index as a prediction variable.

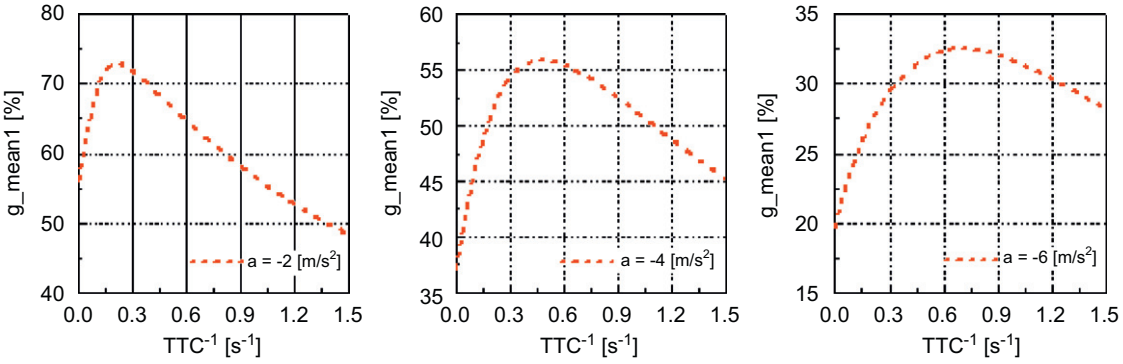

Fig. 11. g_mean_1 computed for three acceleration values (-2, -4, and $-6\,m/s^2$) with the inverse TTC as a prediction variable.

threshold, iT_{th}, is greater than 0.21. Therefore, the warning threshold and the inverse TTC threshold can be used to determine the driving mode. As summarized in Table 3, the threshold values of the warning index are determined as $\alpha_1 = 1.19$, $\alpha_2 = 0.81$ and the threshold values of the inverse TTC are determined as $iT_1 = 0.21$, $iT_2 = 0.49$.

3. Evaluation of adaptive cruise control with a collision avoidance system

The proposed control strategy is compared with manual driving of human drivers. The performance of the subject vehicle under the proposed control strategy is investigated via simulations using real data on driving. The desired clearance is computed by using the clearance model of each driver. The zero-speed clearance, c_0, and the linear coefficient, τ, can be identified and tuned for individual drivers. In this study, the minimum clearance and the linear coefficient are estimated by using the least-squares method on the manual-driving data for each human driver, and the computed parameters are used in the control algorithm. The ACC/CA vehicle behaviors that are similar to manual driving are obtained by using the tuned control parameters.

Fig. 12 presents comparisons between human-driver manual driving ('Human') and controlled behavior ('ACC/CA') in the case of vehicle-following at low speeds in busy urban traffic. The data on the preceding vehicle and the human driver that are shown in Fig. 12 are measured values, and the ACC/CA data are simulated under the same traffic situation. Comparisons of the clearance, accelerations between manual driving and the ACC/CA are shown in Fig. 12(b) and (c), respectively. As shown in Fig. 12, the speed, clearance, and accelerations of the 'ACC/CA' are similar to those of manual driving. The warning index, the inverse TTC, and the mode indicating the driving situation are shown in Fig. 12(d).

About 103 datasets are measured at low-speed and deceleration-driving situations. The traffic situation is reconstructed using the measured data for the preceding vehicle and the ACC/CA data are simulated under the same traffic situation. Tables 4 and 5 summarize comparisons of the acceleration-distribution between the manual-driving data and the ACC/CA data under the situations of stop-and-start and deceleration-to-stop, respectively, on a congested highway and/or dense urban traffic.

These tables show that the ACC/CA controller leads to a similar acceleration-distribution to that of human manual driving in normal-driving situations. Therefore, it is expected that the ACC/CA-controlled vehicle feels natural to the driver in normal-driving situations.

Comparisons between the human driver's manual driving ('Human') and cruise control ('ACC/CA') in the case of severe braking on a high-speed city highway are shown in Fig. 13. The maximum value of the preceding vehicle's deceleration is greater than 8 m/s^2. The data on the preceding vehicle and the human driver that are shown in Fig. 13 are measured values and the 'ACC/CA' data are simulated under the same traffic situation. As shown in Fig. 13, the speed, clearance, and accelerations of the 'ACC/CA' vehicle are similar to those of manual driving. It is shown

Table 4
Comparisons of acceleration characteristics under the stop-and-start situations at low speed

	Acceleration (m/s^2)		
	Preceding	Human	ACC
95%	1.89	1.31	2.02
75%	1.56	1.13	1.38
Mean	1.28	0.95	1.11
25%	1.03	0.83	0.79
5%	0.52	0.40	0.43
Variance	0.17	0.07	0.22

Table 5
Comparisons of acceleration characteristics under the deceleration situations at low speed

	Acceleration (m/s^2)		
	Preceding	Human	ACC
95%	−0.62	−0.45	−0.54
75%	−1.29	−1.17	−1.49
Mean	−1.92	−2.17	−1.87
25%	−2.79	−3.10	−2.58
5%	−3.21	−4.31	−3.12
Variance	0.71	1.5	0.62

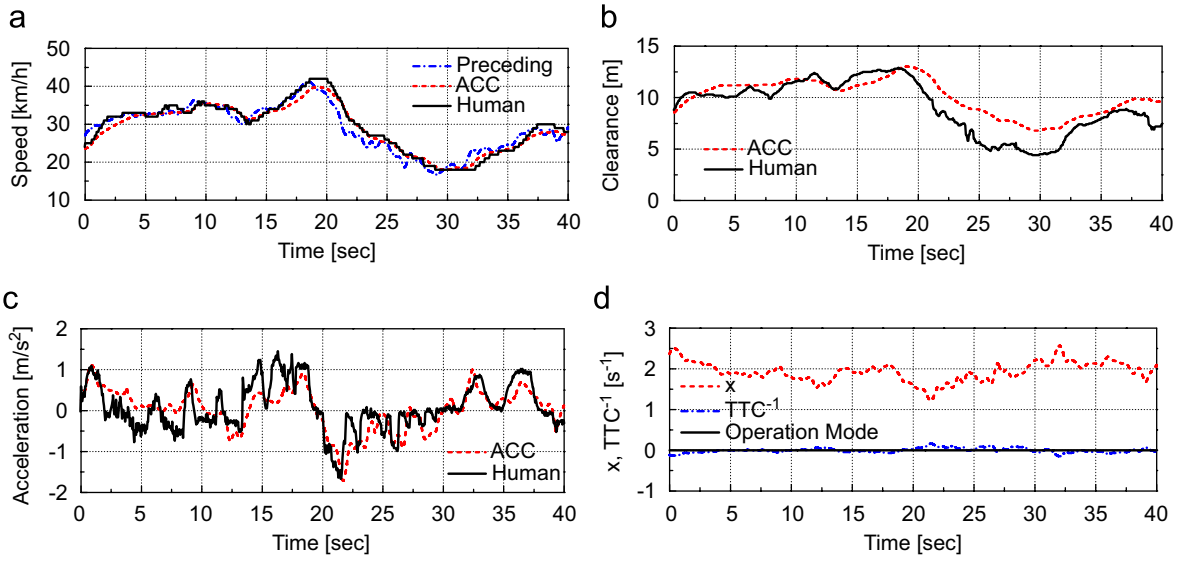

Fig. 12. Comparisons between ACC/CA control and human driving at low speed: (a) vehicle velocity, (b) clearance, (c) acceleration, and (d) indexes and control mode.

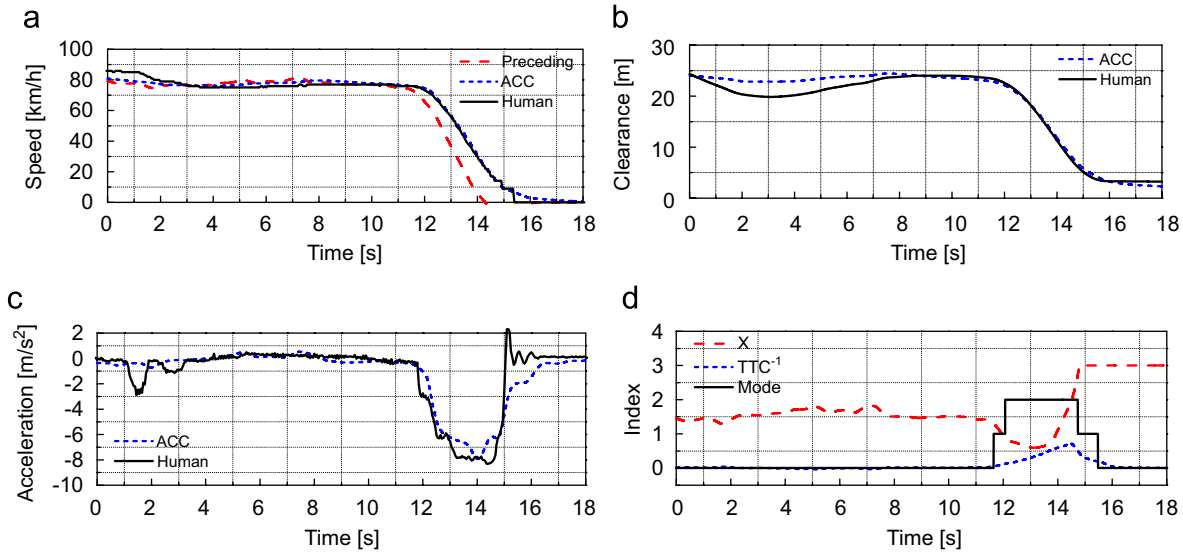

Fig. 13. Comparison between ACC/CA control and human driving in a severe-braking situation on a high-speed city highway: (a) vehicle velocity, (b) clearance, (c) acceleration, and (d) indexes and control mode.

Fig. 14. Configuration of the test vehicle.

in Fig. 13(b) that the proposed control algorithm can keep the vehicle-to-vehicle distance at a safe level in severe-braking situations. Time histories of the warning index, the inverse TTC, and the control mode are compared in Fig. 13(d). The 'Mode' in Fig. 13(d) shows a severe-braking situation, i.e., a 'dangerous' mode. It should be noted from Fig. 13(d) that the severe-braking mode is determined based on the warning index at high speed, and the inverse TTC at low speed, respectively.

4. Vehicle test

Fig. 14 shows a test vehicle, a Hyundai-motors 'Azera,' which is used in this study. The test vehicle is equipped with a laser radar, a longitudinal accelerometer, an ESC module, wheel speed sensors, caliper pressure-sensors for each wheel, etc. Further, the engine RPM, turbine speed of the torque converter, throttle position, and gear status are obtained from the engine control unit via CAN.

The integrated ACC/CA system, including upper-level and lower-level controllers, is implemented by dSPACE hardware (Micro-AutoBox). It manipulates the throttle actuator by sending EMS to voltage level. In addition, it applies the brake to the test vehicle by sending the brake command to the ESC controller, which is connected with the vehicle's ESC module through CAN communication.

Vehicle-following tests were conducted using two vehicles: a preceding vehicle and the subject vehicle. Test results in low-speed driving situations are shown in Fig. 15. The driver turns on the ACC/CA system at 7.5 s and the ACC/CA system automatically controls the subject vehicle. A comparison of vehicle speeds is shown in Fig. 15(a). The desired and actual clearances are compared in Fig. 15(b). Although the velocity of the preceding vehicle fluctuates between 20 and

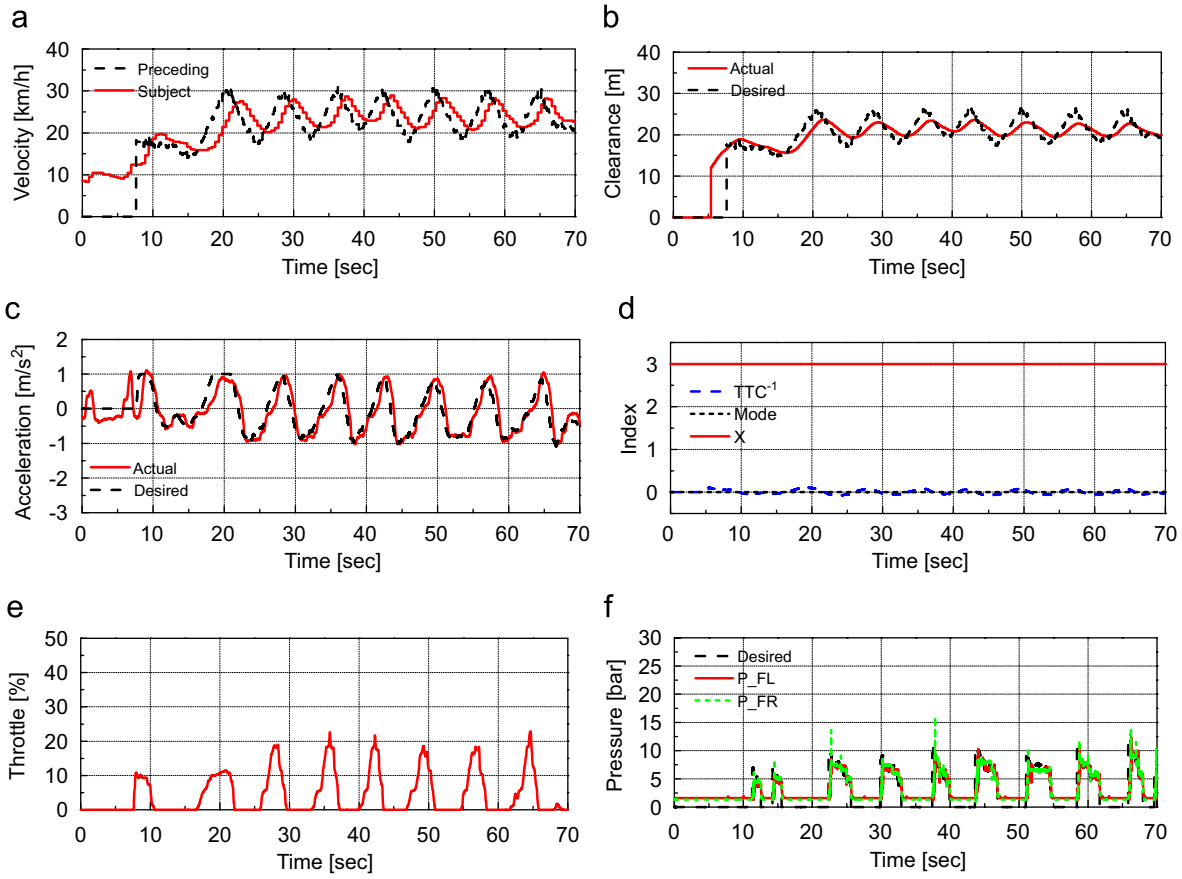

Fig. 15. Vehicle test results: cruise control at low speed: (a) vehicle velocity, (b) clearance, (c) acceleration, and (d) indexes and control mode, (e) throttle angle, and (f) brake pressure.

30 km/h, the subject vehicle follows the velocity of preceding vehicle and, at the same time, maintains the clearance policy. The desired and actual accelerations of the subject vehicle are compared in Fig. 15(d). It can be seen from Fig. 15 that the acceleration of the subject vehicle very closely tracks the desired acceleration profile and ranges between -1 and 1 m/s^2 to improve the quality of the ride. A throttle position sensor (TPS) has been used for measuring the throttle angle. The warning index, the inverse TTC, and the control mode shown in Fig. 15(e) indicate that the current driving situation is safe.

Vehicle test results in SG driving situations are shown in Fig. 16. A comparison of vehicle velocities is shown in Fig. 16(a). When a driver switches from manual to automatic control at 12 s, there are initial differences in the clearance and velocity as shown in Fig. 16(a) and (b), which cause a large jump in the desired acceleration. To prevent the driver from feeling uncomfortable, an upper-level controller of the ACC/CA system restricts the desired acceleration as shown in Fig. 16(c).

The warning index, the inverse TTC, and the control mode shown in Fig. 16(e) indicate that the current driving situation is safe.

Fig. 17 shows the experimental results for a low-speed driving situation with a cut-in vehicle. A time gap of 2.5 s and 5 m of minimum clearance are used in the cut-in test. When the velocity of the subject vehicle is 45 km/h, the preceding vehicle, at a velocity of 35 km/h, suddenly moves into the lane of the subject vehicle after a time-lapse of 60.8 s. The vehicle velocities and clearances are compared in Fig. 17(a) and (b), respectively. As indicated in Fig. 17(e) and (f), when the cut-in vehicle appears, the throttle angle is set to zero and the brakes are applied to reduce the velocity and increase the clearance. Then, the ACC/CA controller activates the throttle actuator to increase the velocity of the subject vehicle so that the relative velocity converges to zero. Fig. 17(d) shows that the warning index decreases, the inverse TTC slowly increases, and the control mode changes from ‘safe-mode’ to ‘warning-mode.’

Fig. 18 shows that the ACC/CA vehicle achieves safety from collision. The initial vehicle velocity is 70 km/h and a cut-in vehicle, at a velocity of 30 km/h, appears in front of the subject vehicle after a time-lapse of 27 s. The initial clearance between the subject and cut-in vehicles is about 30 m. The vehicle velocities and clearance are compared in Fig. 18(a) and (b), respectively. As shown in Fig. 18(c), the acceleration of the ACC/CA vehicle ranges to -6 m/s^2 to avoid collision with the rear-end of the cut-in vehicle. As indicated in Fig. 18(e) and (f), the throttle angle is set to zero and the brakes are applied to reduce the velocity and increase the clearance. Fig. 18(d) shows that the warning index decreases, the inverse TTC abruptly increases, and the control mode changes from ‘safe-mode’ to ‘dangerous-mode.’

5. Conclusion

An integrated algorithm for a full-range ACC system with CA was presented. The control algorithm was designed to achieve behavior of the subject vehicle that would seem natural to a human driver in normal-driving situations and to achieve safe behavior in severe-braking situations in which large decelerations

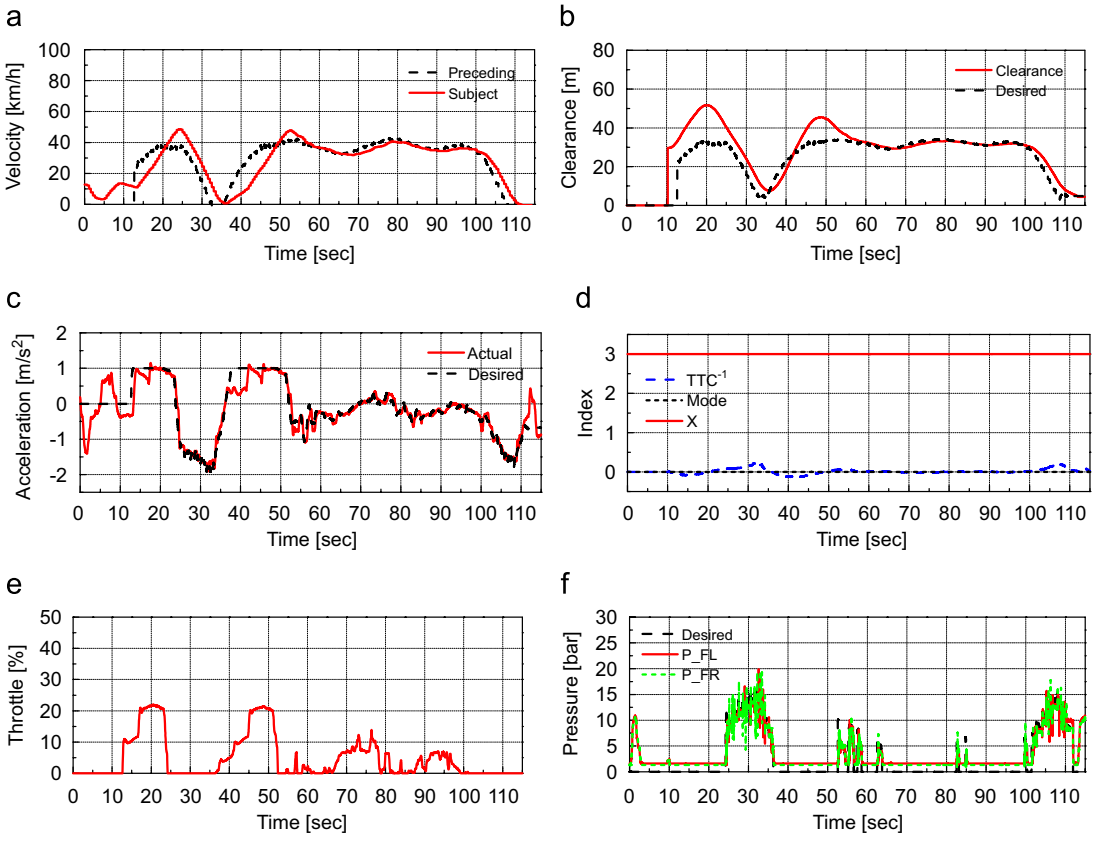

Fig. 16. Vehicle test results: a stop-and-go case: (a) vehicle velocity, (b) clearance, (c) acceleration, and (d) indexes and control mode, (e) throttle angle, and (f) brake pressure.

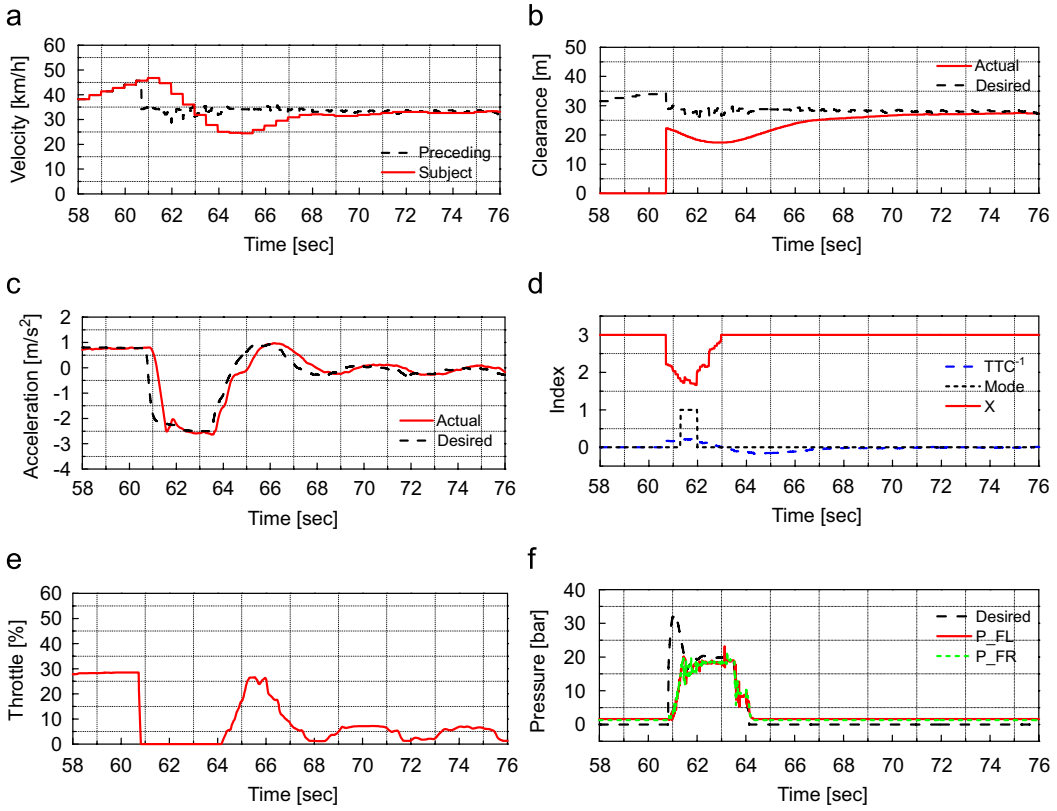

Fig. 17. Vehicle test results: a normal cut-in case: (a) vehicle velocity, (b) clearance, (c) acceleration, and (d) indexes and control mode, (e) throttle angle, and (f) brake pressure.

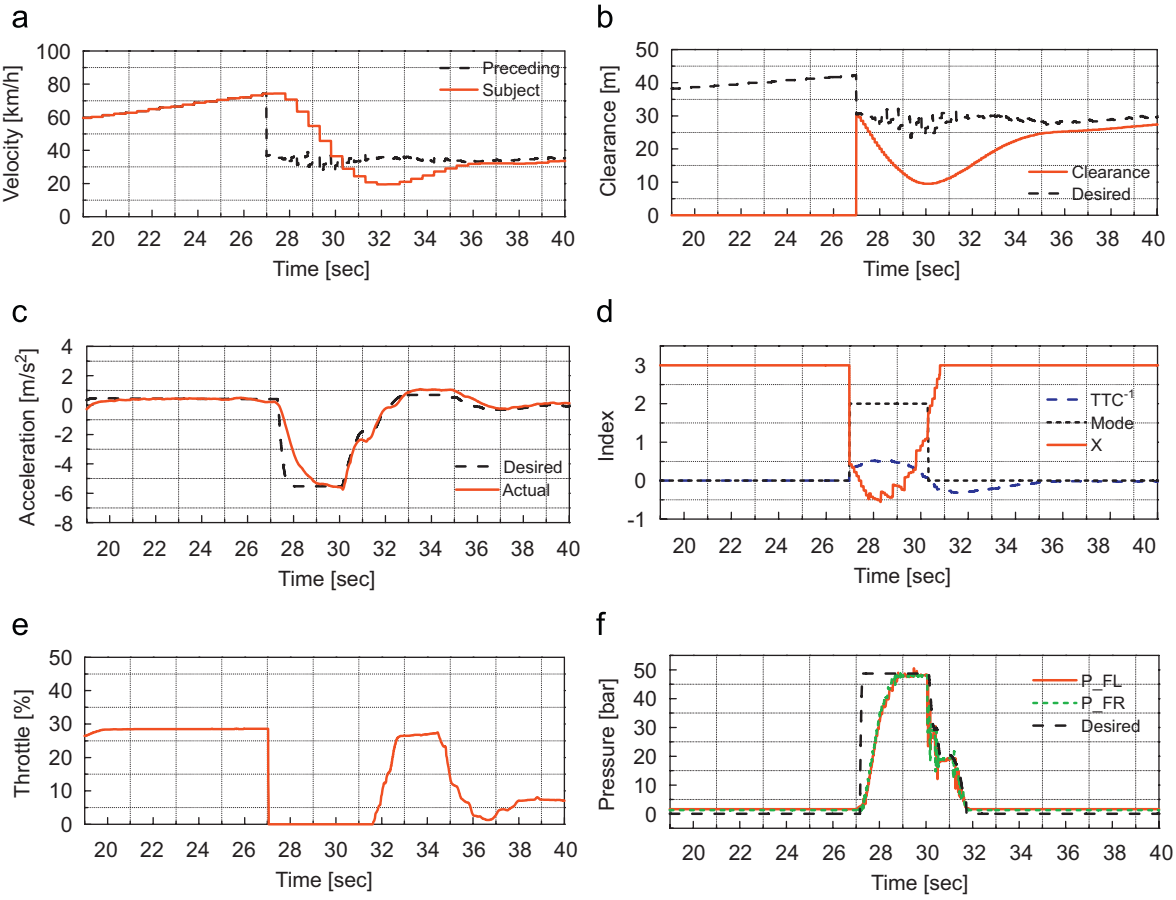

Fig. 18. Vehicle test results: a severe cut-in case: (a) vehicle velocity, (b) clearance, (c) acceleration, and (d) indexes and control mode, (e) throttle angle, and (f) brake pressure.

are necessary. To integrate the ACC and CA systems, the proposed algorithm makes the subject vehicle operate in three modes: comfort, large-deceleration, and severe-braking. While in "comfort-mode (Control Mode-1)", the control objective is to maintain the safety distance from the preceding vehicle while making the process seem natural to the driver. If the driving situation, based on indexes, is determined to be a "large-deceleration mode (Control Mode-2)", the ACC/CA system informs the driver by giving a warning signal and then decelerates. In the case of a dangerous situation, the ACC/CA system switches to the "severe-braking mode (Control Mode-3)," and generates emergency-braking to completely avoid a rear-end collision in vehicle-following situations. To simultaneously ensure driver acceptance and CA performance, the threshold values for the warning index and inverse TTC for each control mode are determined based on manual-driving data, including those in normal-driving and severe-braking situations. The control scheme was evaluated by using real-world, vehicle-driving data. Further, the ACC/CA system was implemented using a test vehicle. It has been shown that the proposed control strategy can provide a natural following performance that is similar to human manual-driving at both high-speed driving and low-speed SG situations, and can prevent the vehicle-to-vehicle distance from dropping to an unsafe level in severe-braking situations. The vehicle longitudinal-control algorithm presented in this study can be a good solution for enhancing driver acceptance of an integrated, full-range ACC/CA system. Strategy tuning, control threshold value tuning, and experimental verification for different road conditions, are the future areas of our research to extend the applicability of the proposed control method.

Acknowledgments

This work is jointly supported by Mando and Hyundai Motor Company.

References

Börner, M., & Isermann, R. (2006). Model-based detection of critical driving situations with fuzzy logic decision making. *Control Engineering Practice*, *14*(5), 527–536.

Fancher, P., Bareket, Z., & Ervin, R. (2000). Human-centered design of an ACC-with-braking and forward-crash-warning system. In: *Proceeding of AVEC2000*. Ann Arbor, MI, USA.

Fancher, P., Bareket, Z., Ervin, R., & Peng, H. (2004). Relationships between manual driving and driving with adaptive cruise control. In: *Proceedings of AVEC2004, 7th international symposium on advanced vehicle control*. Arhnem, The Netherlands.

Goodrich, M. A., & Boer, E. R. (2003). Model-based human-centered task automation: A case study in ACC system design. *IEEE Transactions on Systems, Man and Cybernetics Part A: Systems and Humans*, *33*(3), 325–335.

Han, D., & Yi, K. (2006). Design and evaluation of intelligent vehicle cruise control systems using a vehicle simulator. *International Journal of Automotive Technology (IJAT)*, *7*(3), 377–383.

Hoffmann, E., & Mortimer, R. (1996). Scaling of relative velocity between vehicles. *Accident Analysis and Prevention*, *28*(4), 415–421.

Iljima, T., et al. (2000). Development of an adaptive cruise control system with stop-and-go capability. *SAE Transaction*, Paper no. 2000-01-1353.

Larson, R., & Fowler, G.F. (2005). Driver crash avoidance behavior: Analysis of experiment data collected in NHTSA's vehicle antilock brake system (ABS) research program. *SAE Technical Papers* 2005-01-0423.

Lee, K., & Peng, H. (2004). Data-based evaluation and design of automotive collision warning/collision avoidance algorithm. In: *Proceeding of the AVEC2004, 7th international symposium on advanced vehicle control*, pp. 637–642.

Moon, S., & Yi, K. (2008). Human driving data-based design of a vehicle adaptive cruise control algorithm. *Vehicle System Dynamics*, *8*(4), 111–123.

Peng, H. (2002). Evaluation of driver assistance systems-A human centered approach. In: *Proceedings of the. AVEC*2002 6*th international symposium on advanced vehicle control*, Japan.

Seiler, P., Song, B., & Hedrick, J. K. (1998). Development of a collision avoidance system. *SAE Conference*, 97–103.

Shladover, S. E. (1991). Longitudinal control of automotive vehicles in close-formation platoons. *ASME Journal of Dynamic Systems Measurement and Control*, *113*(2), 231–241.

Vahidi, A., & Eskandarian, A. (2003). Research advances in intelligent collision avoidance and adaptive cruise control. *IEEE Transactions on Intelligent Transportation Systems*, *4*(3), 143–153.

Venhovens, P., et al. (2000). Stop and go cruise control. In: *Proceedings of the Seoul* 2000 *FISITA World Automotive Congress*, Seoul, Korea.

Wang, J., & Rajamani, R. (2004). Should adaptive cruise control systems be designed to maintain a constant time gap between vehicles. *IEEE Transactions on Vehicular Technology*, *53*(5), 1480–1490.

Yi, K., & Moon, I. (2004). A driver-adaptive stop-and-go cruise control strategy. In: *Proceedings of the IEEE international conference on networking, sensing and control*, Taipei, Taiwan.

Yi, K., Woo, M., Kim, S., & Lee, S. (1999). A study on a road-adaptive CW/CA algorithm for automobiles using HiL simulations. *JSME International Journal Series C*, *42*(1), 163–170.